

Intermediate-phase method for computing the natural band offset between two materials with dissimilar structures

Hui-Jun Gu,^{1,2} Yue-Yu Zhang,^{1,2} Shi-You Chen,³ Hong-Jun Xiang,^{1,2} and Xin-Gao Gong^{1,2}

¹Key Laboratory for Computational Physical Sciences (MOE), State Key Laboratory of Surface Physics, Department of Physics, Fudan University, Shanghai 200433, China

²Collaborative Innovation Center of Advanced Microstructures, Nanjing University, Nanjing 210093, China

³Key Laboratory of Polar Materials and Devices (MOE), East China Normal University, Shanghai 200241, China



(Received 11 April 2018; revised manuscript received 29 May 2018; published 12 June 2018)

The band offset between different semiconductors is an important physical quantity determining carrier transport properties near the interface in heterostructure devices. Computation of the natural band offset is a longstanding challenge. We propose an intermediate-phase method to predict the natural band offset between two structures with different symmetry, for which the superlattice model cannot be directly constructed. With this method and the intermediate phases obtained by our searching algorithm, we successfully calculate the natural band offsets for two representative systems: (i) zinc-blende CdTe and wurtzite CdS and (ii) diamond and graphite. The calculation shows that the valence band maximum (VBM) of zinc-blende CdTe lies 0.71 eV above that of wurtzite CdS, close to the result 0.76 eV obtained by the three-step method. For the natural band offset between diamond and graphite which could not be computed reliably with any superlattice methods, our calculation shows that the Fermi level of graphite lies 1.51 eV above the VBM of diamond using an intermediate phase. This method, under the assumption that the transitivity rule is valid, can be used to calculate the band offsets between any semiconductors with different symmetry on condition that the intermediate phase is reasonably designed.

DOI: [10.1103/PhysRevB.97.235308](https://doi.org/10.1103/PhysRevB.97.235308)

I. INTRODUCTION

The band offset between two semiconductors is a vital quantity determining the carrier transport and quantum confinement in heterojunctions, and thus the behavior of any devices based on heterojunctions, such as solar cells, light-emitting diodes, and other optoelectronic devices [1]. Accurate determination of the band offset is therefore critical to the design of heterojunction devices which contain interfaces between two or more semiconductors. Large efforts have been made in the past few decades to develop methods for measurement and calculation of the band offset.

X-ray photoemission spectroscopy (XPS) is often used experimentally to probe core states and hence provides a reference from which the alignment between the valence bands of two systems can be measured [2]. Inspired by this procedure, Wei and Zunger [3] developed the core-level alignment method, where the band offset between two hypothetical compounds L and R is given by

$$\Delta E_v(L/R) = \Delta E_{v,C^*}^R - \Delta E_{v,C}^L + \Delta E_{C,C^*}^{L/R}. \quad (1)$$

Here, $\Delta E_{v,C^*}^R$ and $\Delta E_{v,C}^L$ are the core level to the valence band maximum (VBM) energy separations obtained by bulk calculations for pure R and L , respectively, and $\Delta E_{C,C^*}^{L/R}$ is the core-level difference between L and R under a common energy reference, which is calculated at the L/R superlattice. Here the volume deformation influence on $\Delta E_{C,C^*}^{L/R}$ when building the superlattice is neglected, so this method can only be applied to systems with a small lattice mismatch [4–6]. In order to take the effect of volume deformation into account, Li *et al.* developed

the absolute deformation potential (ADP) correction method [1,7,8], where the VBM states are corrected by $a_{\text{VBM}} \frac{\Delta V}{V}$. Here, a_{VBM} is the VBM absolute volume-deformation potential computed through the procedure proposed by Li *et al.* [7,8], and $\frac{\Delta V}{V}$ is the fractional volume change. Since the calculation of a_{VBM} is practically applicable only to high-symmetry systems and the correction is only up to the linear term of the deformation, this method is proved to be accurate only for high-symmetry systems with a small lattice mismatch.

In order to extend the core-level alignment method to systems with a larger lattice mismatch and low symmetry, Lang *et al.* [9] proposed the three-step method. In this method, in order to calculate the core-level alignment $\Delta E_{C,C^*}^{L/R}$ between L with lattice constants (a_1, a_2, a_3) and R with lattice constants (b_1, b_2, b_3) , the following three steps are used. First, stretch L along the $[100]$ direction to L' with lattice constants (b_1, a_2, a_3) (if $a_1 > b_1$, L will be compressed) and calculate $\Delta E_{C,C'}^{L/L'}$ at the L/L' superlattice. Second, stretch L' along the $[010]$ direction to L'' with lattice constants (b_1, b_2, a_3) and calculate $\Delta E_{C',C''}^{L'/L''}$ at the L'/L'' superlattice. Third, calculate $\Delta E_{C'',C^*}^{L''/R}$ at the L''/R superlattice. In each step, each layer of the superlattice has entirely matched in-plane lattice constants and there is no volume-deformation problem when building the superlattice. From the above procedure, the valence band offset between L and R is given by

$$\begin{aligned} \Delta E_v(L/R) = & \Delta E_{v,C^*}^R - \Delta E_{v,C}^L + \Delta E_{C,C'}^{L/L'} \\ & + \Delta E_{C',C''}^{L'/L''} + \Delta E_{C'',C^*}^{L''/R}. \end{aligned} \quad (2)$$

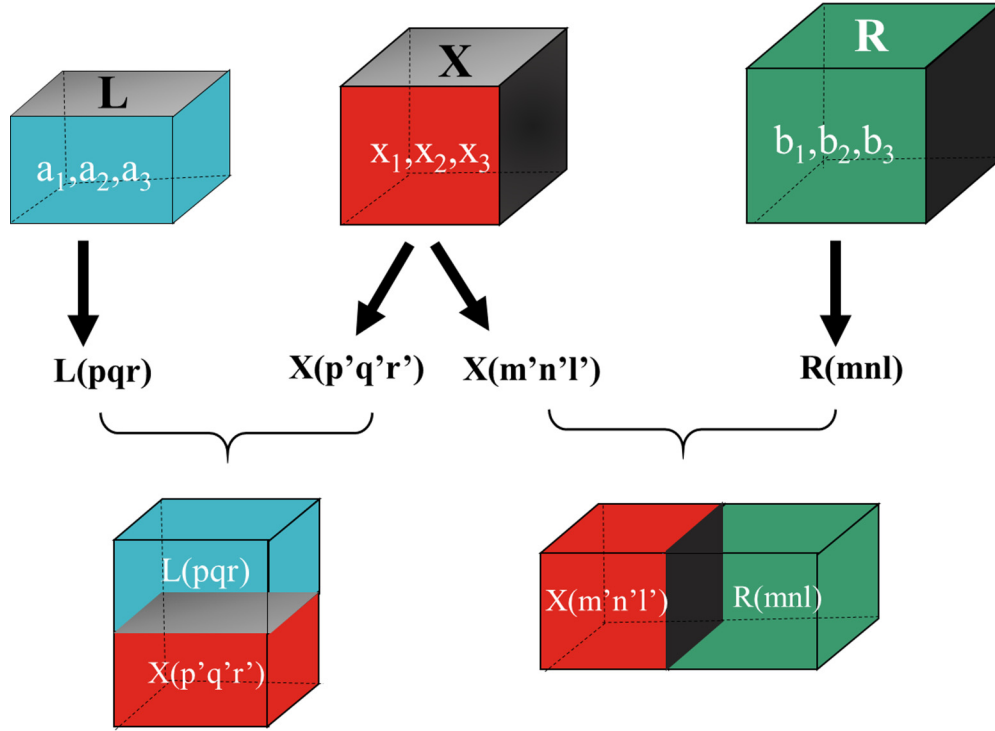


FIG. 1. Schematic illustration of the intermediate-phase method for the natural band offset calculation between L and R . X is an intermediate phase. Letters in brackets are surface indexes.

The validity of the three-step method is guaranteed by the transitivity rule for systems with lattice-matched interfaces [10],

$$\Delta E_v(A/C) = \Delta E_v(A/B) + \Delta E_v(B/C). \quad (3)$$

The transitivity rule assures that for surface-matched systems, such as AlAs/GaAs/Ge, the band offset is intrinsically a bulk property. But for some complicated systems with different lattice symmetry, building an ideal heterostructure is nearly impossible. For instance, with diamond and graphite structures, it is difficult to build a perfect diamond/graphite heterostructure that preserves the bulk property on either side. In this case, the effect of the interface on the band offset is non-negligible and the three-step method is not applicable.

In this paper, we put forward a general method called the intermediate-phase method. By combining this method with the previously proposed three-step method, in principle, we can calculate the natural band offset between any two semiconductors no matter how different their structures are. To test this approach, we first calculate the band offset between Si and Ge as a benchmark, and the obtained result is in good agreement with the three-step method and also with experiments. Then we perform a structure search and find an intermediate phase for calculating the band offset between the zinc-blende CdTe and wurtzite CdS, which are widely used in thin-film solar cell devices. Furthermore, we also find an intermediate phase for calculating the band offset between diamond and graphite, which is unsolvable with previous methods.

In the rest of the paper, we first introduce the intermediate-phase method in detail, and then present the benchmark and application results of this method.

II. INTERMEDIATE-PHASE METHOD

The schematic diagram of the intermediate-phase method is shown in Fig. 1. For any two structures denoted as L and R , we can create an intermediate phase X with a surface $X(p'q'r')$ that symmetrically matches $L(pqr)$ and another surface $X(m'n'l')$ that symmetrically matches $R(mnl)$ with some lattice adjustment if necessary. Then we calculate the band offset between L and X , and between R and X , through the three-step method. Finally, we get the band offset between L and R by

$$\Delta E_v(L/R) = \Delta E_v(L/X) + \Delta E_v(X/R). \quad (4)$$

Obviously, the intermediate phase between L and R is not unique; however, all the different intermediate phases yield approximately the same value for $\Delta E_v(L/R)$, subject to the condition that all the interfaces are well built, so that the transitivity rule is satisfied, and thus the band offset is still a bulk property. Intermediate phases can be constructed easily when the structures of L and R are simple, while in many cases finding a proper intermediate phase is a significant challenge. A good intermediate phase shall have the following properties: low binding energy, large band gap (so that the electrons are localized and have smaller tendency to transfer across the interface), and good structural and constituent match with the two end-point structures (i.e., L and R). Here we propose an algorithm based on differential evolution (DE)

to search for intermediate phases [11,12]. According to the expected properties, the fitness function is defined as

$$f_{\text{bulk}} = f_{\text{bulk}}^{\text{bonding}} + f_{\text{bulk}}^{\text{nonbonding}} = \sum_{ij} \varepsilon_1 \left[\left(\frac{\overline{d_{ij}}}{d_{ij}} \right)^{12} - 2 \left(\frac{\overline{d_{ij}}}{d_{ij}} \right)^6 \right] + \sum_{pq} e^{-k_1(d_{pq} - \overline{d_{pq}})}, \quad (5)$$

$$f_{\text{boundary}} = \sum_{\text{interface}} (f_{\text{boundary}}^{\text{bonding}} + f_{\text{boundary}}^{\text{nonbonding}}) = \sum_{L/X, R/X} \left\{ \sum_{xy} \varepsilon_2 \left[\left(\frac{\overline{d_{xy}}}{d_{xy}} \right)^{12} - 2 \left(\frac{\overline{d_{xy}}}{d_{xy}} \right)^6 \right] + \sum_{uv} e^{-k_2(d_{uv} - \overline{d_{uv}})} \right\}, \quad (6)$$

$$\min f_{\text{total}} = \min (f_{\text{bulk}} + f_{\text{boundary}}). \quad (7)$$

The lattice constants and the number of atoms of the intermediate phase are fixed during each round of the searching process. The atomic positions added with periodic boundary conditions are evolved according to the fitness function. For simplicity, the atomic interactions in the fitness function are divided into two classes: bonding atoms and nonbonding atoms. As a simple example, consider NaCl, in which Na and Cl are bonding atoms while Na and Na, Cl and Cl are nonbonding atoms. The f_{bonding} is inspired by the Lennard-Jones potential and $f_{\text{nonbonding}}$ describes the repulsive interaction. The final fitness function f_{total} consists of two parts: f_{bulk} and f_{boundary} . f_{bulk} describes the distribution of atoms inside the unit cell. The bonding atoms (with atomic distance d_{ij}) are supposed to keep in the optimal distance ($\overline{d_{ij}}$), while nonbonding atoms (with atomic distance d_{pq}) are supposed to keep away from each other by at least the shortest distance $\overline{d_{pq}}$. Since the size of the unit cell is fixed and the atomic distance functions are set, the atoms tend to keep in the best coordination states spontaneously during the optimization process. Similarly, f_{boundary} represents the matching degree of the interfaces. In the function f_{boundary} , d_{xy} is the distance between bonding atoms in the interface and $\overline{d_{xy}}$ is the optimal distance value; d_{uv} is the nonbonding atomic distance in the interface and $\overline{d_{uv}}$ is the shortest distance between them. Minimizing f_{boundary} prompts one surface of the intermediate phase to match with the surface of structure L and another one to match with the surface of R . The coefficients ε_1 , k_1 and ε_2 , k_2 are adjustable parameters that control the weight of each term.

In order to enhance the searching efficiency of the optimization algorithm, we can choose to fix some surface atoms or add certain symmetry rules to decrease the degrees of freedom. If the chosen search parameters do not lead to a satisfactory result, we can choose different surfaces or change the size of the unit cell and try again. Since the searching space is infinite and one can continue to change the searching conditions for multiple attempts, in principle a reasonable intermediate phase can always be designed.

III. BENCHMARK AND APPLICATION OF THE INTERMEDIATE-PHASE METHOD

The structural relaxation and electronic structure calculations are performed based on the density functional theory (DFT) method. The ion-electron interaction is treated by the projector augmented-wave (PAW) technique [13], as implemented in the Vienna *ab initio* simulation package (VASP) [14]. The exchange-correlation potential is treated with the Perdew-Burke-Ernzerhof (PBE) functional [15]. The plane-wave basis-set cutoff is 500 eV. The k mesh is generated by the Monkhorst-Pack scheme [16], and the spacing of k points is approximately $0.03 \times 2\pi \text{ \AA}^{-1}$.

To verify the validity of the intermediate-phase method, we first calculate the valence band offset of a well-known system, the Si/Ge heterostructure. Si and Ge both have the zinc-blende structure with a lattice mismatch of less than 6%, and thus the three-step-method is suitable here. In the first and second steps, we stretch the Si lattice along the [100] and [010] directions, respectively, to make its (001) surface match with the Ge (001) surface. In the last step, we build a heterostructure with stretched Si (001) and Ge (001) surfaces. We finally obtain that the VBM of Ge is 0.689 eV above that of Si. Then we use the present intermediate-phase method to recalculate the band offset. We take the intermediate phase simply as an alloy of Si and Ge with Si:Ge = 1:1 in the zinc-blende structure. For the sake of generality, we choose a different pair of surfaces to build heterostructures with the intermediate phase: Si (001) and Ge (111), which cannot form a heterostructure directly. The result shows that the VBM of Ge lies 0.680 eV above that of Si, which is very close to the 0.689 eV obtained by the three-step method. Experimental measurement shows that the valence band offset of the Si/Ge heterostructure is 0.770, 0.760, and 0.670 eV for 35, 42, and 52% Ge in the relaxed SiGe substrate [17]. Here, the intermediate-phase method leads to a similar result to that of the three-step method and is comparable with experimental results. The present calculation confirmed that the calculated band offset between Si and Ge is indeed a bulk property, irrespective of whether an intermediate phase is adopted or which surfaces we choose. From another perspective, the Si (001) and Ge (111) surfaces have totally different symmetry, which cannot form an interface without defects, while with our present method we can overcome this problem and derive the band offset between Si and Ge using these two surfaces.

We further apply the intermediate-phase method to the CdTe/CdS system and compute the band offset. CdTe is one of the leading thin-film photovoltaic materials due to its ideal band gap and high absorption coefficient [18]. CdS is also widely used as an n -type buffer layer material in thin-film solar cells, and the record efficiency of the thin-film CdTe/CdS solar cell is as high as 22% [19]. Besides the intrinsic nature of the material, the interface property is also of great importance to the efficiency of the photovoltaic devices. The natural band offset between CdTe and CdS is a vital parameter in the interface design. The stable crystal structure of CdTe is zinc-blende (ZB), while that of CdS is wurtzite (WZ). The CdTe (ZB) (111) surface matches CdS (WZ) (001) surface symmetrically, thus one can calculate the band offset using the three-step method directly and the result shows that the VBM of CdTe (ZB) is 0.76 eV above that of CdS (WZ), while

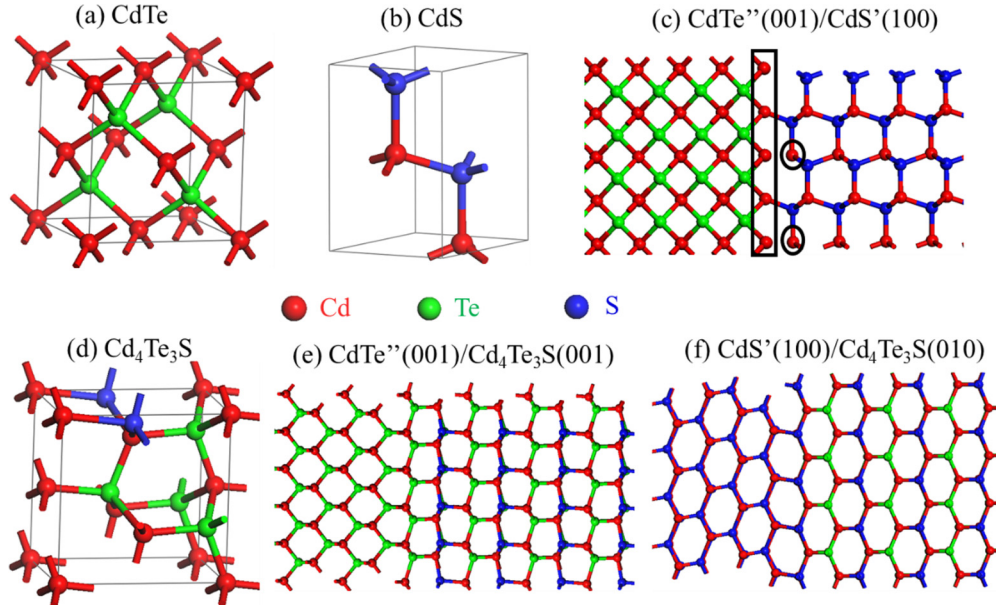


FIG. 2. Bulk structures of (a) CdTe (zinc-blende), (b) CdS (wurtzite), and (d) the intermediate phase $\text{Cd}_4\text{Te}_3\text{S}$, and heterostructures of (c) $\text{CdTe}''(001)/\text{CdS}'(100)$, (e) $\text{CdTe}''(001)/\text{Cd}_4\text{Te}_3\text{S}(001)$, and (f) $\text{CdS}'(100)/\text{Cd}_4\text{Te}_3\text{S}(010)$. Red, green, and blue spheres represent Cd, Te, and S atoms, respectively. Atoms having dangling bonds are indicated with black lines in (c).

for other more general surfaces, such as CdTe (ZB) (001), it can hardly match any surface of CdS (WZ). With the present intermediate-phase method, we can overcome this constraint in surface choosing and pick any pair of surfaces to conduct band offset calculations.

Here we choose the CdTe (ZB) (001) surface and the CdS (WZ) (100) surface to calculate the band offset. These two surfaces have different symmetry, different elemental components, and different polarity; the CdTe (ZB) (001) surface is terminated solely with either Cd or Te atoms, while the CdS (WZ) (100) surface has equal numbers of Cd and S atoms. Thus, constructing an interface directly with these two surfaces brings about many dangling bonds, as shown in Fig. 2(c), which would cause significant charge transfer across the interface. To address this issue, we adopt an alloy obtained by the searching program, $\text{Cd}_4\text{Te}_3\text{S}$, as the intermediate phase. The $\text{Cd}_4\text{Te}_3\text{S}$ (001) surface can match the CdTe (ZB) (001) surface perfectly after deforming the CdTe (ZB) (001) surface from $6.63 \times 6.63 \text{ \AA}$ to $5.40 \times 6.84 \text{ \AA}$. Then, similarly, we have the $\text{Cd}_4\text{Te}_3\text{S}$ (010) surface formed by Cd and S atoms that can match the CdS (WZ) (100) surface after stretching the CdS (WZ) (100) surface from $4.21 \times 6.84 \text{ \AA}$ to $5.40 \times 6.84 \text{ \AA}$. The structures of crystals and interfaces are plotted in Fig. 2. The lattice parameters of CdTe (ZB) and CdS (WZ) are optimized by the PBE calculation and are listed in Table I. The

computational procedure is schematically shown in Fig. 3(a) and the calculated result in Fig. 3(b), with the core level of CdTe (ZB) ($\text{Cd } 1s$) set to be 0 eV. Through the entire process, there are five steps of core-level alignment calculation, and in each step we build a heterojunction. The final result shows that the VBM of CdTe (ZB) lies 0.71 eV above that of CdS (WZ), close to the result (0.76 eV) from the direct three-step method. The deviation of the results possibly lies in the internal electric field caused by the interfacial dipole, which will be discussed in the next section.

To further verify our calculated result, we apply the three-step method to the system of CdTe (ZB)/CdS (ZB) and obtain the valence band offset of 0.81 eV, which is a little larger than that of the CdTe (ZB)/CdS (WZ) system, indicating that the VBM of CdS (WZ) lies a little higher than that of CdS (ZB), which agrees well with the calculated result $\Delta E_v[\text{CdS}(\text{WZ}) - \text{CdS}(\text{ZB})] = 0.046 \text{ eV}$ obtained by Wei and Zhang [20]. Niles *et al.* [21] have performed a photoemission study of a CdS (ZB) layer grown under severe tensile strain on CdTe (ZB) and determined the valence band offset, $\Delta E_v[\text{CdTe}(\text{ZB}) - \text{CdS}(\text{ZB})] = 0.65 \text{ eV}$. Fritsche *et al.* [22] reported the valence band offset of 0.94 eV obtained by photoelectron spectroscopy at the polycrystalline CdTe/CdS heterojunction. Our calculated natural band offset provides a reference value for experiments.

TABLE I. Lattice parameters (\AA), PBE band gaps (eV), and space group of CdTe, CdS, and the intermediate phase $\text{Cd}_4\text{Te}_3\text{S}$. All three structures are direct band-gap semiconductors. The lattice parameters of CdTe and CdS are fully optimized by the PBE calculations.

	a	b	c	α	β	γ	PBE band gap	Space group
CdTe	6.63	6.63	6.63	90	90	90	0.57	$F\bar{4}3m$ [216]
CdS	4.21	4.21	6.84	90	90	120	1.10	$P6_3mc$ [186]
$\text{Cd}_4\text{Te}_3\text{S}$	5.40	6.84	6.84	90	90	90	0.84	Pm [6]

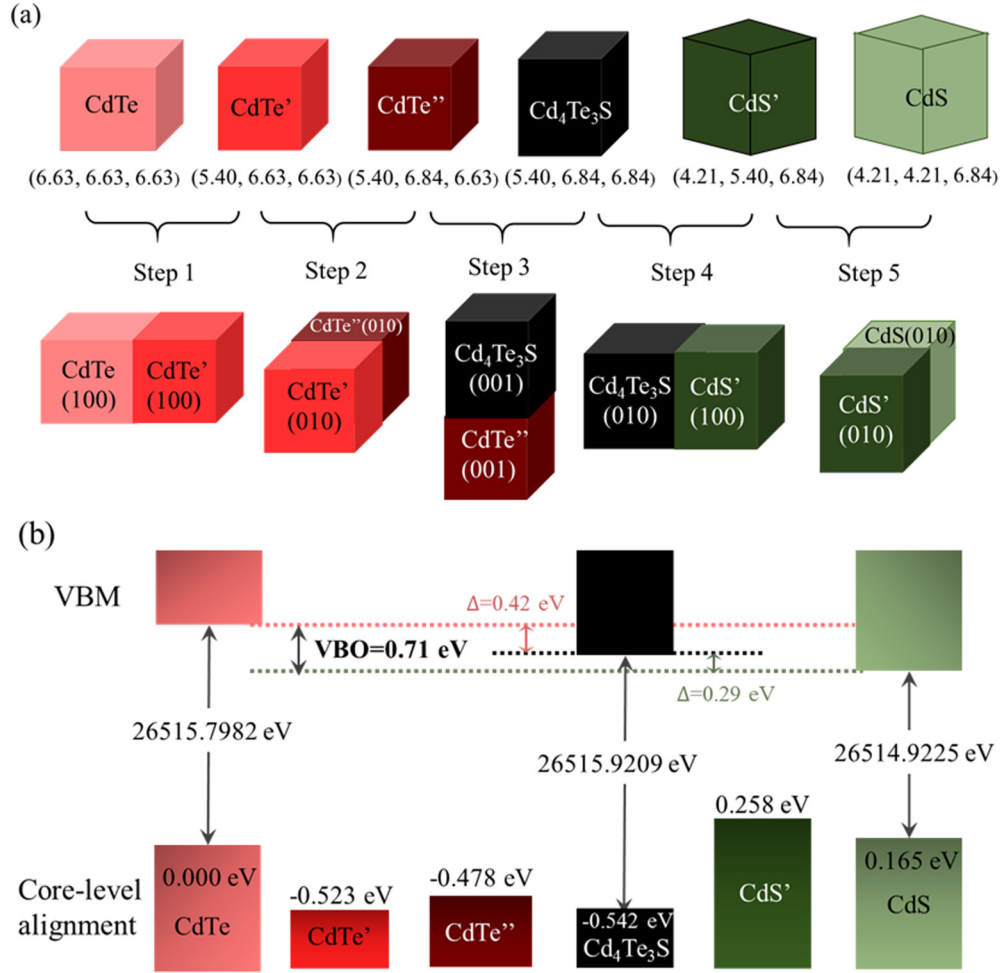


FIG. 3. (a) The procedures for calculating the valence band offset between CdTe (ZB) and CdS (WZ) using the intermediate phase Cd₄Te₃S. In the first, second, and fifth steps, we stretch (or compress) the lattice of CdTe or CdS to make it match with Cd₄Te₃S. In the third and fourth steps, we build heterostructures of Cd₄Te₃S/CdTe'' and Cd₄Te₃S/CdS', respectively. Lattice constants (Å) are listed below the sketch models of crystals. (b) The calculated results of core-level alignment in each step and the valence band offset between CdTe and CdS with the core level of CdTe (Cd 1s) set to be 0 eV.

After demonstrating the validity of the intermediate-phase method through two examples, Si/Ge and CdTe/CdS, we now apply it to compute the band offset between diamond and graphite, which cannot be computed reliably with any previous method. Diamond and graphite are the most common allotropes of carbon. They have very different symmetry and different bonding types, sp^3 and sp^2 hybridization, respectively. Thus, forming an interface with these two structures directly seems unlikely and the previous methods are not applicable, while with the present method, we can calculate the natural band offset between these two structures using

an intermediate phase. Here we adopt an allotrope of carbon obtained by our searching program as the intermediate phase, which has 16 carbon atoms in a unit cell, and so we name it C-16 (see Table II for the structure information). The intermediate phase C-16 has a hexagonal lattice and layered structure, and thus it can form a layered heterostructure with graphite, and its (001) surface can match the diamond (111) surface after compressing the diamond (111) surface from 5.05×5.05 Å to 4.93×4.93 Å. With the intermediate phase C-16, we find that the Fermi level of graphite is 1.51 eV higher than the VBM of diamond (see Fig. 4). Cui *et al.* [23] proposed the surface

TABLE II. Lattice parameters (Å), PBE band gaps (eV), and space group of diamond, graphite, and the intermediate phase C-16. Diamond and C-16 show indirect band gaps. The lattice parameters of diamond and graphite are fully optimized by the PBE calculations.

Name	<i>a</i>	<i>b</i>	<i>c</i>	<i>A</i>	<i>β</i>	<i>γ</i>	PBE band gap (direct/indirect)	Space group
Diamond	3.57	3.57	3.57	90	90	90	4.59/4.12	$Fd\bar{3}m$ [227]
Graphite	2.47	2.47	7.83	90	90	120	0.00/0.00	$P6_3/mmc$ [194]
C-16	4.93	4.93	7.90	90	90	120	1.19/1.09	Cm [8]

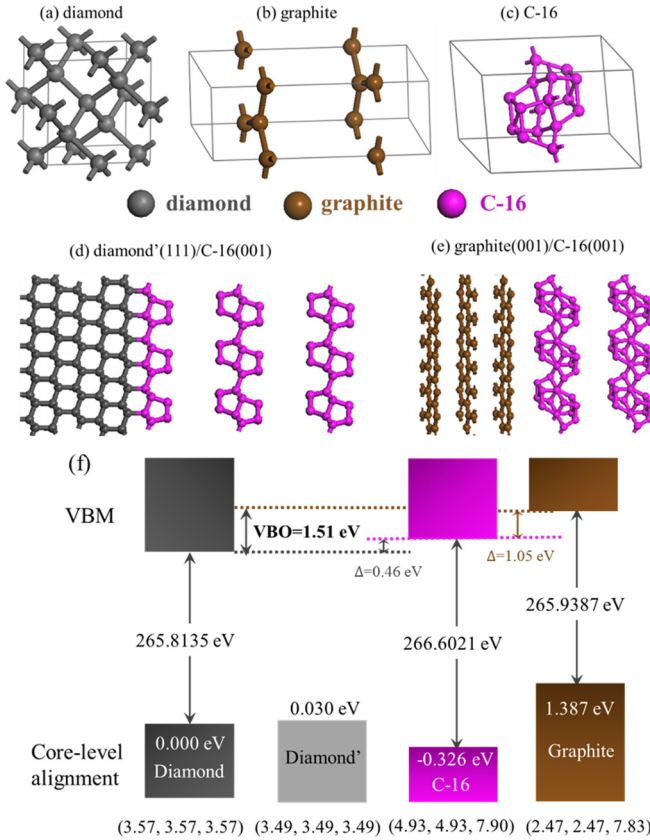


FIG. 4. Bulk structures of (a) diamond, (b) graphite, and (c) the intermediate phase C-16 and heterostructures of (d) diamond'(111)/C-16(001) and (e) graphite(001)/C-16(001). Gray, brown, and violet spheres represent the carbon atoms in diamond, graphite, and C-16, respectively. (f) The calculated results of core-level alignment and the band offset between diamond and graphite with the core level of diamond (C 1s) set to be 0 eV. The core-level alignment between diamond and diamond' is obtained through the three-step method. Lattice constants (Å) are listed below the rectangles.

graphitization of the diamond (111) surface when annealing the diamond at 1400 K, and suggested an offset of 1.42 eV from the VBM of diamond to the Fermi level of graphite, which agrees well with our results.

IV. DISCUSSION

The dominant error with the superlattice model comes from the internal electric field across the heterostructure. The electric field is mainly caused by two contributions: (1) the intrinsic

polarity of the surface [for example, the CdTe (ZB) (111) surface is terminated solely with either Cd or Te ions so that the surface is not neutral], and (2) interfacial charge transfer forming a dipole near the interface. The internal electric field can change the electrostatic potential on either side of the heterojunction and shift the value of core-level alignment. To reduce the effect of this electric field, one should (i) choose intermediate phases with a larger band gap so that the electrons are relatively localized, (ii) select neutral surfaces as the first choice which can minimize the effect of the electric field, and (iii) build interfaces appropriately without dangling bonds, etc. Only when the influence of the internal electric field is relatively weak is the transitivity rule well satisfied. Then the result obtained from the intermediate-phase method is valid.

V. CONCLUSION

We have proposed the intermediate-phase method to calculate the natural band offset between two materials with different symmetry, for which a direct superlattice cannot be constructed. A simple approach is also presented for the search for the intermediate phases. Compared to previous methods, the present method can be applied to systems with different symmetry and a large lattice mismatch, where the direct construction of a superlattice is unlikely or would produce large structure distortion or charge transfer, thus violating the transitivity rule. For these systems, with our present method one can design an intermediate phase properly and build heterostructures reasonably with target materials so that the transitivity rule can be well satisfied.

We demonstrate the validity of the intermediate-phase method by comparing the calculated band offsets of Si/Ge and CdTe (ZB)/CdS (WZ) obtained by the intermediate-phase method with those obtained by previous methods. For the band offset between diamond and graphite structures, which could not be computed using any previous methods, we adopt a carbon allotrope C-16 as the intermediate phase and determine that the Fermi level of graphite is 1.51 eV higher than the VBM of diamond. One could expect that the present intermediate-phase method opens an avenue for computing the natural band offsets between two materials with different symmetry.

ACKNOWLEDGMENTS

This work was supported by the Special Funds for Major State Basic Research (2016YFB0700701, 2016YFA0301001), National Natural Science Foundation of China (NSFC), Program for Professor of Special Appointment (Eastern Scholar), and the Qing Nian Ba Jian Program.

- [1] Y.-H. Li, A. Walsh, S. Chen, W.-J. Yin, J.-H. Yang, J. Li, J. L. F. Da Silva, X. G. Gong, and S.-H. Wei, *Appl. Phys. Lett.* **94**, 212109 (2009).
- [2] S. P. Kowalczyk, J. T. Cheung, E. A. Kraut, and R. W. Grant, *Phys. Rev. Lett.* **56**, 1605 (1986).
- [3] S. H. Wei and A. Zunger, *Appl. Phys. Lett.* **72**, 2011 (1998).
- [4] S. Chen, X. G. Gong, and S.-H. Wei, *Phys. Rev. B* **75**, 205209 (2007).

- [5] S. Chen, A. Walsh, J.-H. Yang, X. G. Gong, L. Sun, P.-X. Yang, J.-H. Chu, and S.-H. Wei, *Phys. Rev. B* **83**, 125201 (2011).
- [6] Q. Shu, J.-H. Yang, S. Chen, B. Huang, H. Xiang, X.-G. Gong, and S.-H. Wei, *Phys. Rev. B* **87**, 115208 (2013).
- [7] Y. H. Li, X. G. Gong, and S. H. Wei, *Appl. Phys. Lett.* **88**, 042104 (2006).
- [8] Y.-H. Li, X. G. Gong, and S.-H. Wei, *Phys. Rev. B* **73**, 245206 (2006).

- [9] L. Lang, Y.-Y. Zhang, P. Xu, S. Chen, H. J. Xiang, and X. G. Gong, *Phys. Rev. B* **92**, 075102 (2015).
- [10] C. G. Van de Walle and R. M. Martin, *Phys. Rev. B* **35**, 8154 (1987).
- [11] Y. Y. Zhang, W. G. Gao, S. Y. Chen, H. J. Xiang, and X. G. Gong, *Comp. Mater. Sci.* **98**, 51 (2015).
- [12] Y.-Y. Zhang, S. Chen, H. Xiang, and X.-G. Gong, *Carbon* **109**, 246 (2016).
- [13] P. E. Blochl, *Phys. Rev. B* **50**, 17953 (1994).
- [14] G. Kresse and J. Furthmüller, *Comp. Mater. Sci.* **6**, 15 (1996).
- [15] J. P. Perdew, K. Burke, and M. Ernzerhof, *Phys. Rev. Lett.* **77**, 3865 (1996).
- [16] H. J. Monkhorst and J. D. Pack, *Phys. Rev. B* **13**, 5188 (1976).
- [17] J. T. Teherani, W. Chern, D. A. Antoniadis, J. L. Hoyt, L. Ruiz, C. D. Poweleit, and J. Menendez, *Phys. Rev. B* **85**, 205308 (2012).
- [18] S. H. Wei, S. B. Zhang, and A. Zunger, *J. Appl. Phys.* **87**, 1304 (2000).
- [19] M. Gloeckler, I. Sankin, and Z. Zhao, *IEEE J. Photovolt.* **3**, 1389 (2013).
- [20] S. H. Wei and S. B. Zhang, *Phys. Rev. B* **62**, 6944 (2000).
- [21] D. W. Niles and H. Hochst, *Phys. Rev. B* **41**, 12710 (1990).
- [22] J. Fritsche, T. Schulmeyer, D. Kraft, A. Thissen, A. Klein, and W. Jaegermann, *Appl. Phys. Lett.* **81**, 2297 (2002).
- [23] J. B. Cui, J. Ristein, and L. Ley, *Phys. Rev. B* **59**, 5847 (1999).